DIFFUSE INTERSTELLAR BANDS IN REFLECTION NEBULAE

O. FISCHER*, TH. HENNING**, W. PFAU* AND R. STOGNIENKO**

* *University Observatory, Jena, Germany*

** *Research Group of the Max Planck Society, Jena, Germany*

ABSTRACT. Our Monte Carlo code for radiation transport calculations is used to compare the profiles of the $\lambda\lambda$ 5780 and 6613 Ångstrom diffuse interstellar bands in the transmitted and the reflected light of a star embedded within an optically thin dust cloud. In addition, we calculated the behaviour of polarization across the bands. The wavelength dependent complex indices of refraction across the bands were derived from the embedded cavity model. In view of the existence of different families of diffuse interstellar bands the question of other parameters of influence is addressed in short.

1. INTRODUCTION

An important hypothesis for the origin of the diffuse interstellar bands (DIBs) relates these features to impurities in interstellar grains. Shapiro & Holcomb (1986) calculated extinction profiles for grains containing resonantly absorbing impurity atoms or molecules with the so-called embedded cavity model developed by Purcell & Shapiro (1977). Bromage (1972) already noted that not only the extinction but also the scattering (or backscattering) properties of the grains can be used as a sensitive indicator of the DIBs' origin. From an observational point of view, reflection nebulae should be excellent targets to look for differences between DIBs seen in scattered and direct light.

In this contribution, we present the results of radiative transfer calculations obtained with our Monte Carlo code (Fischer et al., 1994). As a model we assume a star embedded in an extended envelope and compute both the DIB profiles expected along the direct line of sight to the star and towards other positions in the nebula. We also investigate the course of polarization across the bands. Our calculations refer to the $\lambda\lambda$ 5780 and 6613 Å bands.

2. OBSERVATIONS

Successful observations of DIBs in the light reflected in the interstellar environment of early-type stars are scarce. A'Hearn (1971) published measurements of the strength of DIB λ 4430 in the light of three reflection nebulae and compared the band strength in the nebular light to the one observed in the illuminating star itself. He used a photoelectric photometer and isolated the band with the aid of narrow-band filters.

For NGC 1435 (the Merope nebula in the Pleiades) and for NGC 2177, he found an increase of the strength of the λ4430 band in the reflected relative to the direct light from the star. In IC 432, however, no difference was recorded. In view of the extreme faintness of the reflection nebulae and the shallowness of the λ4430 feature the results have to be considered with some caution.

Josafatson and Snow (1987) used the DIBs to trace reflection nebulae for their composition. They restricted themselfes, however, to the direct lines of sight to the stars.

3. MODEL

As a first approximation of a reflection nebula, we use a sphere (radius = 5000 AU) with a point-like star in the centre (see Figure 1). The stellar radiation transport through the extended spherical dust shell is calculated under inclusion of multiple scattering effects. Exact Mie scattering characteristics are used. The Stokes parameters of the polarized light coming out of the nebula are recorded in the computer memory as a function of the projected radius in a column vector with 51 elements. The recording is comparable to the results of observations of the nebulae with diaphragms in form of circular rings. The first vector element is situated at the end of the line of sight to the embedded star. Above all, it represents the directly transmitted light. All the other elements cross the dust shell and contain the contribution due to scattered light. Contrary to our model, Bromage (1972) located the illuminating star in front of the nebula and calculated only the backscattered light.

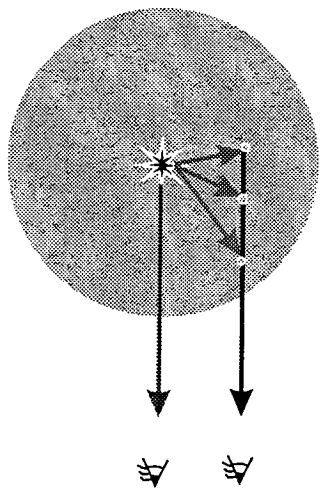

Figure 1: Model configuration.

We investigate two DIB profiles and calculate these at 34 wavelength positions which concentrate to the band centre. We calculate the line extinction A_λ following $A_\lambda = (I_0 - I_\lambda)/I_0$, where I_λ is the line intensity at the wavelength λ and I_0 is the intensity of the continuum near the absorption band. For the determination of I_0 we use three further wavelengths on either side of the bands where $A_\lambda \approx 0$. For each wavelength 10^6 weighted photons are started from the central star whereby a weighting factor equal to one was used in all cases. To introduce a certain spectral distribution of the stellar radiation the results simply have to be weighted.

The optical properties of the spherical dust particles (host grains with impurities) are calculated using the embedded cavity model by Purcell & Shapiro (1977) corresponding to parameter sets given in the paper of Shapiro & Holcomb (1986). The optical constants are summarized together with other model parameters in Table 1. In the present paper we restrict ourselfs to single size particle dust populations with grains of dirty silicate and dirty water ice. The particles are either homogeneously or with a $1/r^2$ law distributed inside the sphere. In addition, we varied the optical depth, $\tau_{\rm ext}$, of the dusty shell (single scattering case: $\tau_{\rm ext} \approx 0.1$ and a case with multiple scattering: $\tau_{\rm ext} \approx 0.5$).

Table 1: Parameters of the model. [1] The wavelength of the DIB is given with the model name, [2] particle radius, [3] complex refractive index of the particles beside but near the band (no influence of the impurities), [4] number density of the dust at the outer edge of the shell, [5] optical depth of the shell beside but near the band.

Model [1]	a [2] [Å]	Material	$n+ik$ [3]	Particle distribution	n [4] [m^{-3}]	$\tau_{\rm ext}$ [5]
5780A	920	dirty silicate	$1.73+i0.07$	homogeneous	0.0104	0.134
5780B	920	dirty silicate	$1.73+i0.07$	homogeneous	0.04	0.517
5780C	690	dirty silicate	$1.74+i0.14$	homogeneous	0.02933	0.134
5780D	690	dirty silicate	$1.74+i0.14$	homogeneous	0.1	0.456
5780E	920	dirty silicate	$1.73+i0.07$	$\sim 1/r^2$, $R_{\rm i}=15$AU	0.00033	0.134
5780F	920	dirty water ice	$1.34+i0.19$	homogeneous	0.101	1.214
5780G	920	dirty water ice	$1.34+i0.19$	homogeneous	0.011	0.132
5780H	1150	dirty water ice	$1.33+i0.09$	homogeneous	0.00573	0.091
5780I	1150	dirty water ice	$1.33+i0.09$	homogeneous	0.03	0.478
6613A	920	dirty silicate	$1.73+i0.07$	homogeneous	0.0104	0.091
6613B	920	dirty silicate	$1.73+i0.07$	homogeneous	0.055	0.4796
6613C	690	dirty silicate	$1.74+i0.14$	homogeneous	0.02933	0.0996
6613D	690	dirty silicate	$1.74+i0.14$	homogeneous	0.15	0.5046
6613E	920	dirty silicate	$1.73+i0.07$	$\sim 1/r^2$, $R_{\rm i}=15$AU	0.00033	0.0905
6613F	1150	dirty water ice	$1.33+i0.09$	homogeneous	0.00573	0.072
6613G	1150	dirty water ice	$1.33+i0.09$	homogeneous	0.04	0.5059

4. RESULTS

In Figure 2 line extinction profiles expected for the direct light to the star and the scattered light from the nebulae (integrated over all radii) are given. The outer continuum wavelengths are omitted from the graphs. The profiles calculated by Shapiro & Holcomb are of course well represented by our models for the direct line of sight. All the profiles of the scattered light split into an absorption and an emission wing. The absorption is slightly shifted from the DIB central wavelength to the blue and the emission wing to the longward side. The effect is due to the course of the scattering efficiency, $Q_{\rm sca}$, shown in Fig 3 versus wavelength.

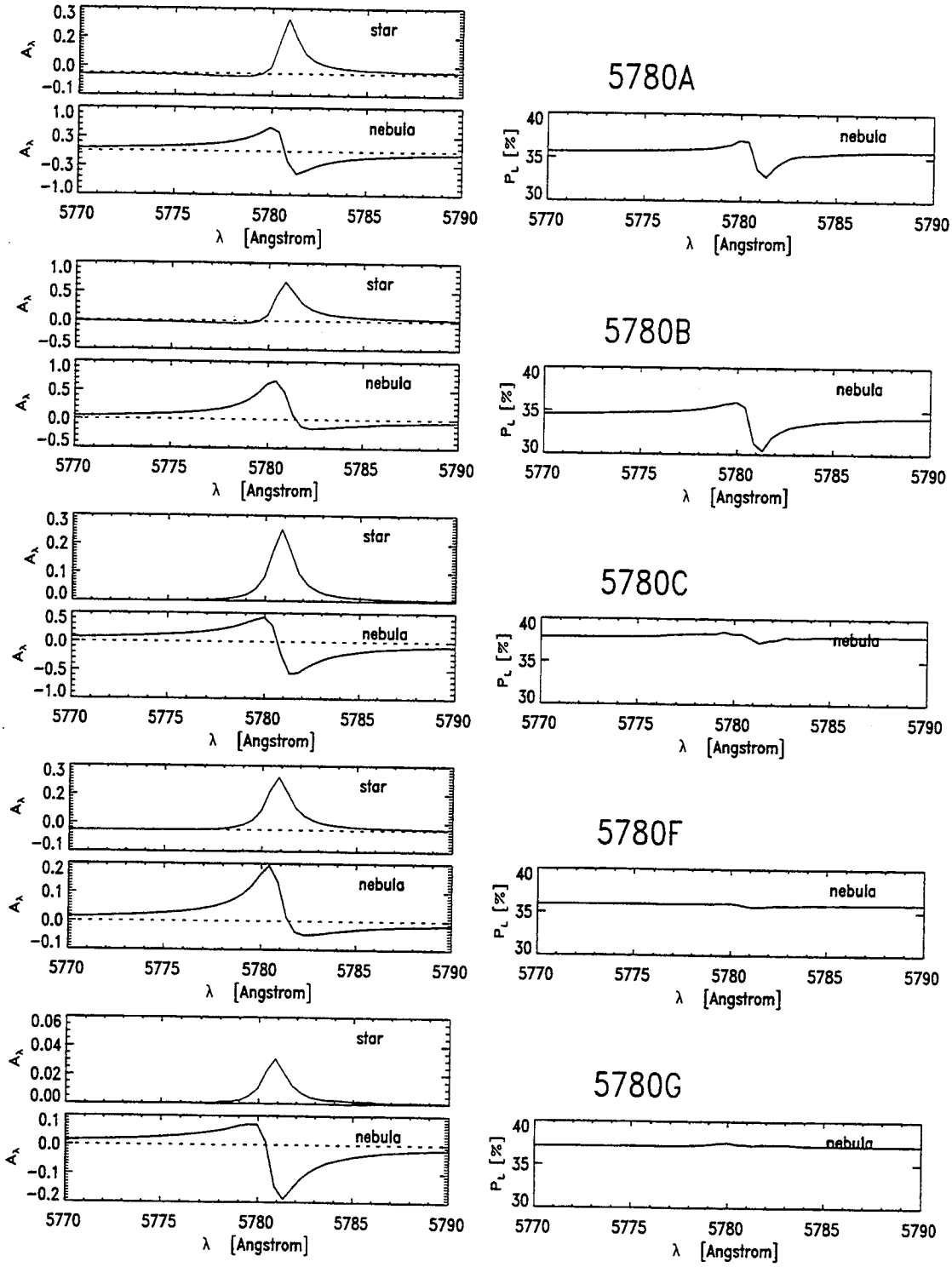

Figure 2: Line extinction A_λ for the direct transmitted light from the star (upper left panel) and the integrated scattered light from the nebulae (lower left panel) and linear polarization P_L (lower right panel) across the $\lambda\lambda$ 5780 band for 5 different parameter sets.

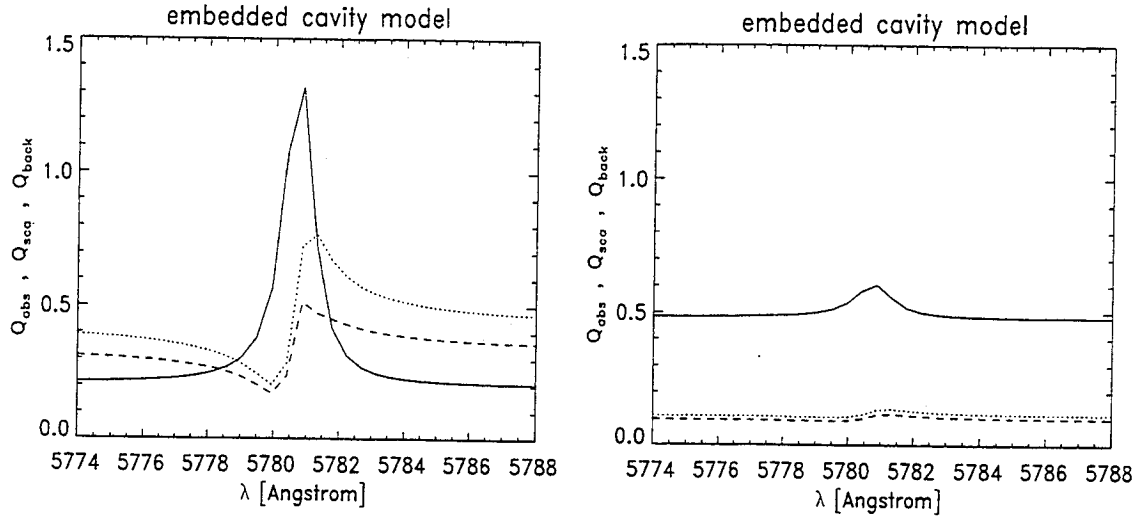

Figure 3: Efficiency factors for absorption ($Q_{\rm abs}$, solid line), scattering ($Q_{\rm sca}$, dotted line) and back scattering ($Q_{\rm back}$, dashed line) versus the wavelength. Left: dirty silicate, $m = 1.73 + i0.07$, $a = 920$Å; right: dirty water ice particle of the same size, $m = 1.34 + i0.19$. The distribution of $Q_{\rm sca}$ implies the characteristics of the DIB 5780 in the scattered light. In comparison to the dirty silicate grains the dirty water ice grains produce a fainter band which is dominated (corresponding to $Q_{\rm sca}(\lambda)$) by the emission wing (see also Figure 2, compare between models 5780A and 5780G) .

With increasing optical depth (multiple scattering) the strength of the emission wing is reduced. Contrary to single scattering in case of multiple scattering the influence of $Q_{\rm sca}(\lambda)$ becomes smaller because of the radiation which is scattered into the line of sight. The relation of the strengths of the wings and their wavelength shift is dependent on the material and size of the particles. In case of dirty water ice particles the emission wing dominates the absorption. From our calculations no significant variations of the band profiles with projected distances between the line of sight and the direction to the star is evident. Therefore, in Figure 2 the integrated nebular light is plotted.

In Figure 2, profiles of the linear polarization $P_{\rm L}$ across the bands are also drawn. From the calculations we find a small variation of the degree of linear polarization of up to about 10%, with the weaker polarization on the red side of the central wavelength. The change of polarization is smaller for more absorbing particles.

The overall behaviour of the bands is similar for the two features DIB 5780 and DIB 6613 considered here.

In comparison to our results, Bromage got splitted bands only for graphite particles but not for the silicate grains. This is due to his model for the determination of the refractive index of the grains containing impurities where he used an other treatment of the interactions between the host material and the impurities and a rather low impurity concentration.

5. CONCLUSION

The presence of red emission wings aside the DIBs in the light of reflection nebulae would be a strong evidence in favour of a dust model as the carrier of the DIB absorbers. Therefore, we plan spectroscopic observations of reflection nebulae and further calculations with particle mixtures and other configurations of reflection nebulae.

REFERENCES

A' Hearn, M. F. 1971, *A. J.*, **76**, 264.
Bromage, G. E. 1972, *Ap. Space Sci.*, **18**, 449.
Fischer, O., Henning, Th., Yorke, H. W. 1994, *Astr. Ap.*, **284**, 187.
Josafatson, K., Snow, T. P. 1987, *Ap. J.*, **319**, 436.
Purcell, E. M., Shapiro, P. R. 1977, *Ap. J.***214**, 92.
Shapiro, P. R., Holcomb, K. A. 1986, *Ap. J.***310**, 872.